J Fluoresc (2014) 24:57–65
DOI 10.1007/s10895-013-1270-2

ORIGINAL PAPER

Enhanced Oxidation Stability of Quasi Core-Shell Alloyed CdSeS Quantum Dots Prepared Through Aqueous Microwave Synthesis Technique

Hong-Ju Zhan · Pei-Jiang Zhou · Rong Ma · Xi-Jing Liu · Yu-Ning He · Chuan-Yun Zhou

Received: 3 May 2013 / Accepted: 14 July 2013 / Published online: 10 August 2013

Abstract Quasi core shell alloyed CdSeS quantum dots (QDs) have been prepared through a facile aqueous-phase route employing microwave irradiation technique. The optical spectroscopy and structure characterization evidenced the quasi core shell alloyed structures of CdSeS QDs. The X-ray diffraction patterns of the obtained CdSeS QDs displayed peak positions very close to those of bulk cubic CdS crystal structures and the result of X-ray photoelectron spectroscopy data re-confirmed the thick CdS shell on the CdSe core. The TEM images and HRTEM images of the CdSeS QDs ascertained the well-defined spherical particles and a relatively narrow size distribution. On the basis, the stability of the obtained QDs in an oxidative environment was also discussed using etching reaction by H_2O_2. The experiments result showed the as-prepared QDs present high tolerance towards H_2O_2, obviously superior to the commonly used CdTe QDs and core-shell CdTe/CdS QDs, which was attributed to the unique quasi core-shell CdSeS crystal structure and the small lattice mismatch between CdSe and CdS semiconductor materials. This assay provided insight to obtain high stable crystal structured semiconductor nanocrystals in the design and synthesis process.

Keywords Quasi core-shell alloyed quantum dots · Oxidation stability · CdSeS quantum dots · Microwave-assisted synthesis

H.-J. Zhan · P.-J. Zhou (✉) · R. Ma · X.-J. Liu · Y.-N. He · C.-Y. Zhou
School of Resource and Environmental Science, Hubei Biomass-Resource Chemistry and Environmental Biotechnology Key Laboratory, Wuhan University, Wuhan 430079, China
e-mail: zhoupj@whu.edu.cn

H.-J. Zhan
e-mail: 2010102050026@whu.edu.cn

H.-J. Zhan
Jingchu University of Technology, Jingmen 448000, China

Introduction

The unique photoluminescence properties of quantum dots (QDs)-narrow and size tunable photoluminescence spectra, broad absorption spectra, high resistance to photobleaching and long fluorescent lifetime—make them attractive alternatives to conventional organic fluorophores in biomedicine and biotechnology [1–3]. When considering the specific application, strategies to obtain QDs that are water-soluble and biocompatible are guided by several criteria [4, 5]: (i) high photoluminescent quantum yield (PLQY), (ii) small size, enabling access to confined biological compartments; (iii) stability of luminescence properties under real operation conditions, (iv) low nonspecific adsorption; and (v) easy functionalization. During the past two decades, there are tremendous efforts made in the synthesis of high-quality QDs with high photoluminescence quantum yield (PL QY) and small size, little attention has been paid to the synthesis of high stable QDs. Once the obtained semiconductor nanocrystals were used in optical applications, the most important issue we should consider is the stability of the nanoparticles under environmental exposure to things such as oxidants [6, 7], light [8–11], acid [12–14] and so on. Hardman reviewed that possibly the most important aspect of QD toxicity is their stability, both in vivo and during synthesis and storage. Under oxidative and photolytic conditions, the core-shell coatings of QD have been found to be labile, degrading and thus exposing potentially toxic "capping" material or intact core metalloid complexes or resulting in dissolution of the core complex to QD core metal components (e.g., Cd, Se), which is the primary cause of toxicity [15]. So far, there are increasing reports on the effect and mechanism of light on the semiconductor nanocrystals, only a lack of emphasis on the influence of oxidative condition. The report of Zhang et al. proved the PL bleaching is directly related to the existence of environmental oxygen molecules in living cells [16]. Mancini et al. also reported

an oxidative process involving neutral-charge molecular such as hypochlorous acid (HOCl) and hydrogen peroxide (H_2O_2) that leads to fluorescence quenching and chemical degradation of polymer-encapsulated QDs [6]. Thus, to obtain highly anti-oxidative QDs remains a challenge before their biological application.

Here we present the facile synthesis and properties of CdSeS QDs with a quasi core-shell alloyed structure. The stability of the as-prepared CdSeS QDs under the oxidative environment was also discussed through the fluorescence spectra, UV/Vis absorption spectra and X-ray photoelectron spectroscopy techniques using H_2O_2 as oxidant. The results showed that these alloyed QDs exhibited obviously enhanced stability than the naked CdTe QDs and core-shell CdTe/CdS QDs.

Experimental

Materials

Cadmium chloride hemipentahydrate ($CdCl_2 \cdot 2.5H_2O$, 99 %), 3-mercaptopropionic acid (MPA, 99 %), selenium powder (Se, 99.8 %), tellurium powder (Te, 99.9 %) and anhydrous sodium sulfite (Na_2SO_3, 97 %) were purchased from Sigma Aldrich. Other routine chemicals such as hydrogen peroxide (H_2O_2, 30 %), potassium borohydride (KBH_4, 99 %), reagent grade ethanol and iso-propanol were all received from Shenshi Chem. Ltd. All the chemicals were used directly without any purification. Ultrapure water (18.2 $M\Omega cm^{-1}$) was used as solvent in all experiments.

Na_2SeSO_3 solution: The preparation of 0.3 mol L^{-1} Na_2SeSO_3 solution has been described by Hankare et al. [17] with some modification. Briefly, 2.3670 g selenium powder (0.030 mol) and 9.453 g sodium sulfite (0.075 mol) were added into a 250 mL three-neck flask with 80 mL ultrapure water and then the mixtures were heated to 90 °C. After 6 h' refluxing, the gray selenium powder disappeared and a light yellow solution was obtained. When cooling down to room temperature naturally, the solution was transferred into a100 ml volumetric flask and brought to volume by ultrapure water, which was used as the stock solution of selenium source in the next stage of the reaction.

Devices

The synthesis of alloyed CdSeS QDs was carried out on a microwave digestion/extraction system (Milestone, Italy) and some exclusive Teflon® inner vessels with a volume of 100 mL were used to ensure security in the reactions demanding high temperature and pressure.

Synthsis of CdSeS QDs

The water-dispersed alloyed CdSeS QDs were prepared by microwave irradiation of $CdCl_2$ and MPA in the presence of Na_2SeSO_3 as selenium source, similar with the method reported by Qian et al.[18]. Typically, a Cd precursor solution was obtained by adding Na_2SeSO_3 solution to an alkaline solution (pH 9.0) containing $CdCl_2$ and MPA. The molar ratio of Cd: MPA: Se used in the precursor solution was 8:20:1 and the typical concentration of Cd was 1.25 mmol L^{-1}. Then 50 mL of the precursor solution was transferred to an exclusive vessel and placed inside the microwave digestion furnace to heat via microwave irradiation. After the reaction was completed, the yellow QDs solution was cooled down to ambient temperature naturally and used to measure UV–vis absorption spectra and fluorescence spectra. The obtained solution was purified by addition of twice the volume of isopropanol and then centrifugation at 12,000 rpm for 10 min. The purified dilute solutions were used to record TEM and high-resolution (HR) TEM images and determine element content on an ICP-AES instrument. The purified concentrated solutions were frozen in a −20 °C refrigerator and then subjected to freeze–dry in a freezedrier (ChristAlpha1-2LD, Germany) to obtain solid samples prior to the analysis of XRD, FTIR and XPS.

Characterization of Alloyed CdSeS QDs

UV/Vis absorption spectra were measured on a Shimadzu UV-1601 Spectrophotometer in a quartz cuvette of 1 cm path length. Fluorescence spectra were recorded on a Hitachi F-4500 spectrophotometer using 354 nm as excitation wavelength. All the optical measurements were conducted under ambient conditions. The PLQYs of the prepared QDs were calculated by comparing the integrated fluorescent emission area with that of Rhodamine 6G in ethanol (PLQY, 89 % [19]) according to the equation described by Crosby et al. [20]. Powder X-ray diffraction (XRD) patterns were collected on a Bruker-Axs D 8 advanced diffractometer with Cu-$K\alpha$ radiation ($\lambda = 1.54178$ Å) to identify the crystal structure. X-ray photoelectron spectroscopy (XPS) analysis was done on a Kratos XSAM-800 apparatus using a monochromatic Mg-$K\alpha$ source at 1253.6 eV. Transmission Electron Microscopy (TEM) and High Resolution Transmission Electron Microscopy (HRTEM) images were taken on a JEOL model JEM 2100 instrument operating at an acceleration voltage of 200 kV. The samples were prepared by dropping the purified dilute QDs solution on the ultrathin carbon film prior to the evaporation of excess solvent. Fourier Transform Infrared Spectroscopy (FT-IR) was obtained on a NICOLET 5700 FT-IR spectrometer through potassium bromide tabletting. Inductively Coupled Plasma Atomic Emission Spectrometry (ICP-AES) was performed on an IRIS Intrepid II XSP spectrometer (Thermo. Electron Corp., USA).

Tolerance Towards Oxidation by H_2O_2

In order to study the stability of CdSeS QDs in an oxidative environment, we investigated the tolerance of the CdSeS QDs against chemical oxidation by H_2O_2 according to the previous report [21] but with some modification. For comparison, naked MPA-capped CdTe QDs, core-shell CdTe/CdS QD_{573} and CdTe/CdS QD_{630} with a thin CdS shell of 0.5 nm and a thick CdS shell of 0.7 nm, respectively, synthesized through microwave irradiation according to the literatures [22, 23] have also been discussed in this study. Before measurement, all the samples were purified using isopropanol to remove the unreacted ions and were adjusted to a concentration with an absorption value of 0.1 at the corresponding excitation wavelength. In the etching experiments, 3 % H_2O_2 (0.025 mL) solution was added to the QD solution (3.0 mL) with stirring under ambient conditions at room temperature. The fluorescence spectra and UV–vis absorption spectra were recorded after different intervals of etching time.

Results and Discussion

Synthesis of Quasi Core Shell Alloyed CdSeS QDs

The water-dispersed quasi core shell alloyed CdSeS nanoparticles were synthesized through microwave irradiation by a one-step procedure. Firstly, selenium anions released from the solution of Na_2SeSO_3 in the alkaline medium reacted with cadmium cations to form CdSe core at relatively low temperature as the following reactions [17, 24].

$$Na_2SeSO_3 + NaOH \rightarrow Na_2SO_4 + NaHSe \quad (1)$$

$$NaHSe + NaOH \rightarrow Na_2Se + H_2O \quad (2)$$

$$CdCl_2 + Na_2SeO_3 + 2NaOH \rightarrow CdSe + Na_2SO_4 + 2NaCl + H_2O \quad (3)$$

Then, sulfide ions released from MPA at high temperature reacted with the excess cadmium cations to form a CdS shell and deposit on the surface of CdSe core to passivate the surface defects [25, 26]. This procedure could also be witnessed from the temporal evolution of the photoluminescence spectra of CdSeS QDs at various heating times (Fig. 1). It could be seen that, when the heating time was short (Fig. 1a, 5 min), the as-prepared QDs displayed obvious trap states emission band at 600 nm and very weak excitonic luminescence peak, so only light red fluorescence emission was observed. As the heating time increased, the trap state luminescence peak became weaker and weaker, until they disappeared completely. Meanwhile, the high energy of excitonic luminescence became stronger and stronger, showed bright green fluorescence. As the heating time was longer than 40 min, a significant drop of fluorescence emission was clearly observed. Similar observations were ascribed to the strain released through the formation of dislocations in the shell with increasing shell thickness, e.g., for core/shell CdSe/ZnS QDs [27–29] and core/shell/shell CdTe/CdS/ZnO QDs [30]. The temperature at which the alloyed QDs are formed is also very critical. At higher temperatures, on one hand, the deposited CdS shell was very thick to cause serious strain between the core and shell that would quench the fluorescence emission; on the other hand, the surface stabilizer would come off from the nanocrystals for the cadmium-chalcogenide bond ruptured, which lead to the particles aggregation of QDs. Overcoating the particles at relatively low temperatures could lead to incomplete passivation of the surface trap state emission and only poor excitonic luminescence was obtained. Through optimizing the experiment conditions, alloyed CdSeS QDs with a maximum PLQY of 30 % were obtained after 40 min microwave irradiation at 130 °C.

Characterization of Alloyed CdSeS QDs

Figure 2 displayed the X-ray diffraction (XRD) patterns of alloyed CdSeS QDs prepared at 130 °C for 10 min and 30 min microwave irradiation. For comparison, the standard XRD pattern of cubic CdSe and CdS are also shown. Both of the samples showed broad peaks, implying that the nanocrystals are very small. Three obvious peaks including (111), (220) and (311) can be clearly observed, proved the high crystallinity with negligible content of the amorphous phase. The diffraction pattern of the QDs obtained at 130 °C for 10 min

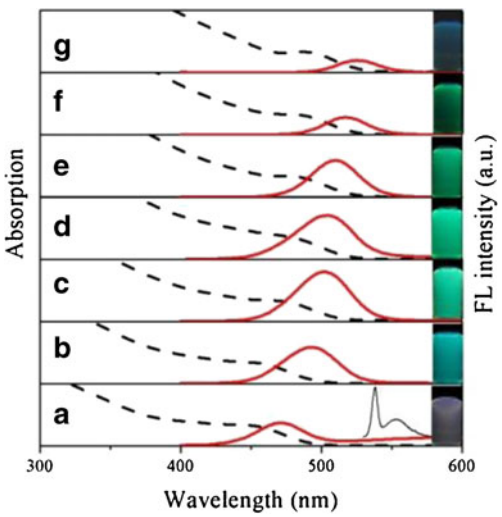

Fig. 1 Temporal evolution of the photoluminescence spectra of CdSeS QDs at various heating times: (**a**) 5 min, (**b**) 15 min, (**c**) 30 min, (**d**) 40 min, (**e**) 50 min, (**f**) 60 min and (**g**) 80 min. The microwave irradiation temperature is 130 °C. The inset shows the details of the photoluminescence spectra of a. The pictures on the right show the photoluminescence of the obtained QDs under a 365 nm UV lamp

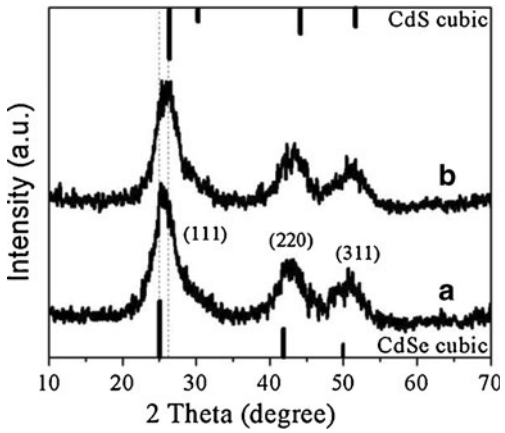

Fig. 2 Powder X-ray diffraction (XRD) patterns of CdSeS QDs obtained at 10 min (**a**) and 30 min (**b**) irradiation, respectively. Standard diffraction lines of cubic CdSe (*bottom*) and cubic CdS (*top*) are also shown for comparison

microwave irradiation was consistent with that of the bulk cubic CdSe structure but slightly shifted toward larger 2θ values and lies between those of bulk cubic CdSe and CdS phase. As for the samples obtained at 130 °C for 30 min microwave irradiation, the diffraction pattern was consistent with that of the bulk cubic CdS structure, indicating that the crystal structures of CdSeS QDs is much closer to that of bulk cubic CdS, agree well with the result reported by Qian et al. even if a different selenium source was used [18].

The transmission electron microscopy (TEM) and high-resolution TEM (HRTEM) images of the alloyed CdSeS QDs were presented in Fig. 3. These images showed that the obtained nanocrystals exhibited spherical shapes with homogeneous size distributions. The results agreed well with the narrow PL full-width at half maximum (FWHM) bandwidth (44 nm). The measured mean sizes were 2.1±0.6 nm, obviously smaller than that of CdSeS QDs obtained from NaHSe (12 nm) [18]. Besides, the lattice fringes were clearly displayed in the HRTEM images, which further verified the high crystallinity of these nanocrystals.

As a sensitive technique for the analysis of the compositions and structures of the surfaces of nanocrystals, XPS was used to analyze the surface state of the obtained alloyed CdSeS QDs. Figure 4 is the typical XPS spectra of the CdSeS QDs where panel a is the survey spectrum and panels b–d are the high-resolution binding energy spectra for Cd 3d, S 2p and Se 3d, respectively. According to the survey spectrum, the elements Cd, Se, S, Na, O and C were all detected, proved the existence of these elements in the sample. The characteristic peaks at 405.1 eV and 411.9 eV were assigned to Cd 3d5 and Cd 3d3, 54.1 eV to Se 3d, 161.9 eV to S 2p, respectively. It is worth noting that the peak S 2p at 161.9 eV could be decomposed into two doublet which located at 162.1 and 163.6 eV, respectively. According to the report of Borchert et al.[31], the peak at 163.6 eV represented the coordination situations of S from the MPA ligand (Cd-SR) and the peak at 162.1 eV from the CdS shell (Cd-S) formed during decomposition of MPA under the effect of microwave irradiation [32, 33]. The absolute predominance in the area of peak at 162.1 eV directly demonstrated that the deposited CdS shell was thick, totally different from that of the common core-shell structured QDs, which re-confirming the quasi core shell alloyed structure, that is, a CdSe-rich core and a thick CdS shell.

In order to determine the chemical composition of the ligands capping on the surface of the alloyed CdSeS QDs, a further characterization of Fourier Transform Infrared Spectroscopy (FT-IR) absorbance measurements of pure MPA and CdSeS QDs was conducted and the results were presented in Fig. 5. Figure 5a represents the FT-IR spectrum of MPA, which displayed a number of characteristic spectral bands such as the stretching vibration of -SH group at 2,562 cm^{-1}, the wagging vibration of S-CH_2- at 1,255 cm^{-1}, the stretching vibration of C-S at 671 cm^{-1} and so on. All of these characteristic bands are also present in the spectrum for the MPA-capped alloyed CdSeS QDs (Fig. 5b) except the characteristic peak at 2,562 cm^{-1} corresponding to the stretching vibration of -SH group in the MPA molecule disappeared. In addition, the C=O band at 1,703 cm^{-1} in the MPA was shifted to the COO^- band at 1,556 cm^{-1}. The above data proved that the Cd-SH complex was formed on the surface of the alloyed CdSeS QDs.

In order to further investigate the formation mechanism, the CdSeS QDs obtained at different reaction time were used to analyze the element content by ICP-AES and the temporal

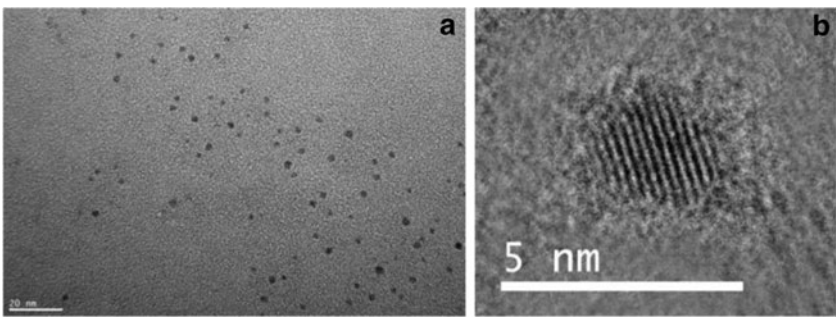

Fig. 3 TEM (**a**) and HRTEM (**b**) images of CdSeS QDs obtained at 130 °C for 30 min microwave irradiation. *Scale bars* are 20 nm (TEM) and 5 nm (HRTEM), respectively

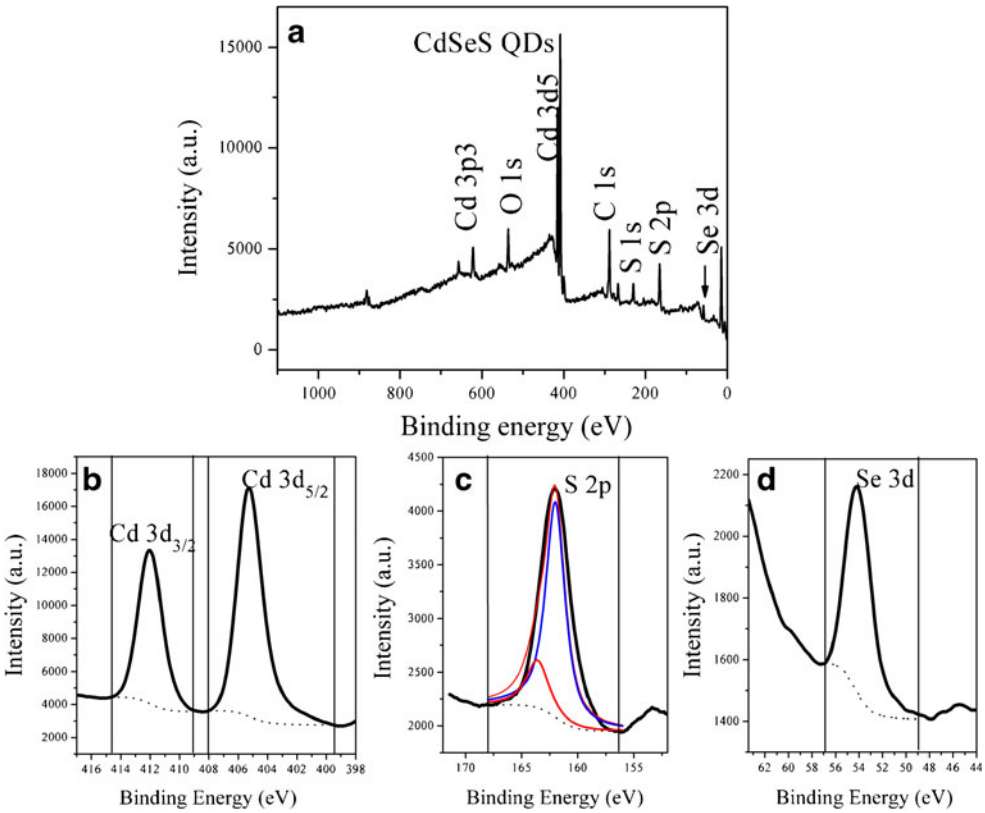

Fig. 4 X-ray photoelectron spectra (XPS) of CdSeS QDs. (**a**) XPS survey spectrum. Binding energy spectra of Cd 3d (**b**), S 2p (**c**) and Se 3d (**d**), respectively

evolution of molar ratio of Cd, S and Se (set Se as 1) was shown in Table 1. When the reaction time was short, the obtained CdSeS QD_{480} displayed low molar ratios of Cd/Se and S/Se, suggesting that the CdSe was the dominant component and S come mainly from the capping MPA. With the reaction time was extended, both molar ratios increased, implying the gradual deposition of CdS shell on the CdSe core as sulfide ions was released from MPA under the microwave irradiation. In the sample of CdSeS QD_{530}, the molar ratio of S/Se was much larger than 6, which indicated that the CdS was the dominant component in the alloyed QDs, that is, the CdSeS QDs was composed of a CdSe core and a thick CdS shell on the surface. The radial increase of CdS content from core to the surface made it difficult to determine the thickness of CdS layer as that of common core-shell QDs. Generally, we can control the shell thickness through adjusting the reaction time and temperature and the optimized thickness endowed CdSeS QDs with the highest fluorescence intensity.

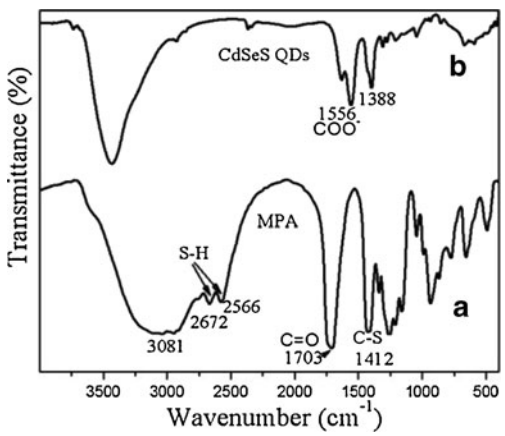

Fig. 5 FT-IR spectra of MPA (**a**) and CdSeS QDs (**b**), respectively

Oxidation Stability

Once released into the environment, QDs may be transformed by various complex changes altering their toxicity and fate such as the redox process. The low content of oxidant under environmental conditions makes the oxidation process slow. In order to speed up the oxidation process under environmental conditions, 3 % H_2O_2 were used to react with QDs solution to investigate their chemical stability. Initially we studied the tolerance of the obtained CdSeS QDs and the common used

Table 1 Temporal evolution of molar ratio of Cd, S and Se characterized by ICP-AES

Items	Cd	S	Se
QD_{480}	2.97	4.93	1
QD_{508}	5.46	6.27	1
QD_{534}	7.61	6.39	1

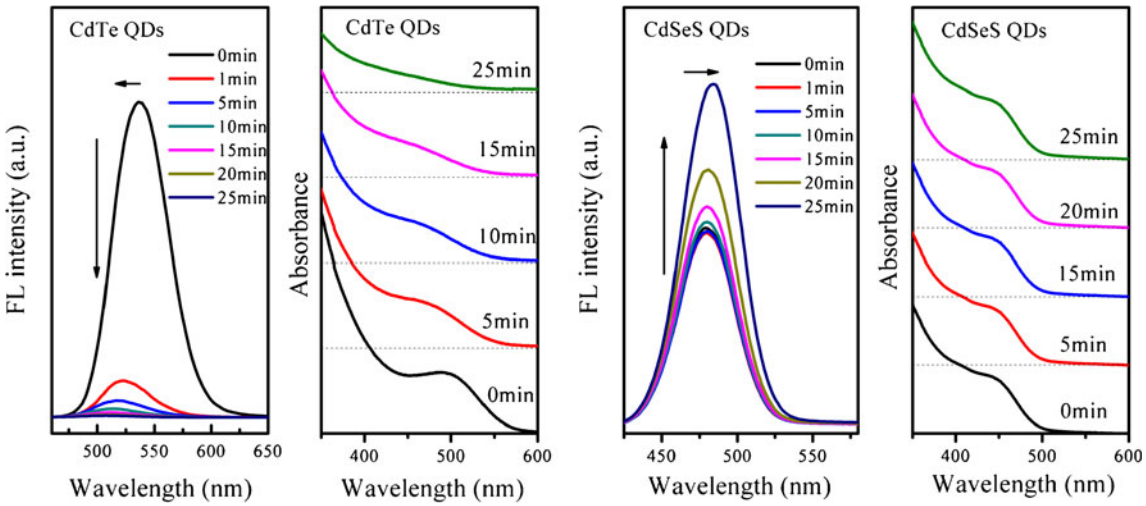

Fig. 6 Time dependence of FL spectra and UV-vis absorption spectra of CdTe QDs and CdSeS QDs against H_2O_2 etching

naked MPA-capped CdTe QDs (about 2.1 nm) by comparison. The synthesis of CdTe QDs was conducted through microwave irradiation and the size was calculated using the first exciton absorption peak position following Peng's method [34]. During the etching experiments, as 3 % H_2O_2 solutions were added to the QDs solutions, respectively, the temporal evolution of fluorescence spectra and UV–vis absorption spectra was recorded and the results were shown in Fig. 6. Clearly, there was an evident decrease in the PL intensity and a significant blue shift in the maximum emission wavelength of CdTe QDs, suggesting a decrease in the diameter due to etching effect of H_2O_2; the first exciton absorption peak disappeared after 25 min etching of H_2O_2 re-confirmed the degradation of the CdTe crystal particles. Comparatively, there was an obvious increase in the PL intensity and a slight red shift in the maximum emission wavelength for the alloyed CdSeS QDs, indicating the oxidation of H_2O_2 exhibited no erosion effect; the nearly intact first exciton absorption peak after 25 min reaction of H_2O_2 also showed the same result. So in all probability, a shell with a lower valence band binding energy was formed on the surface of the alloyed CdSeS QDs after the treatment of H_2O_2. At that time, we attributed the high anti-oxidation property of alloy CdSeS QDs to the shell protection. So core-shell CdTe/CdS QD_{573} and CdTe/CdS QD_{630} with a thin shell of 0.5 nm and a thick shell of 0.7 nm, respectively, were also studied in the oxidation experiments and

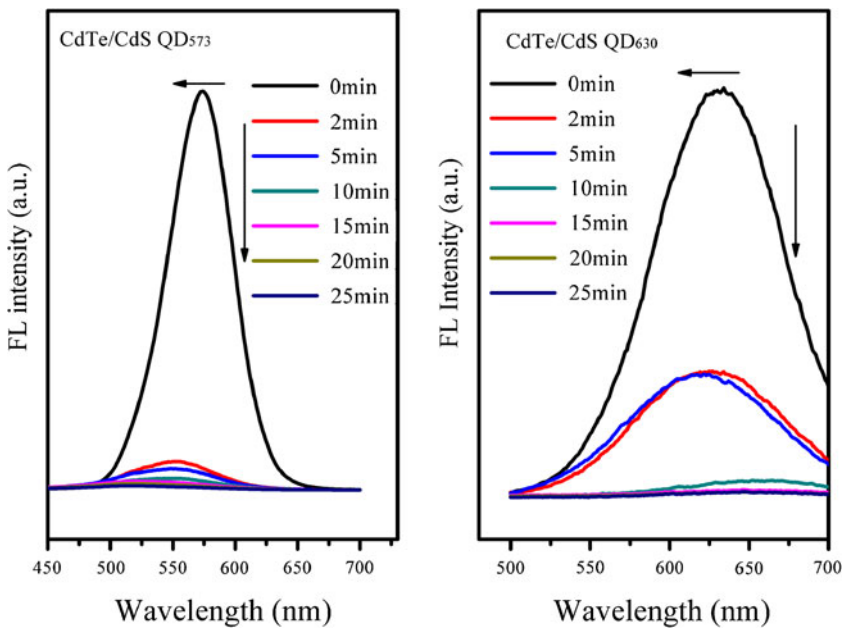

Fig. 7 Time dependence of FL spectra of core-shell CdTe/CdS QD_{573} and CdTe/CdS QD_{630} against H_2O_2 etching

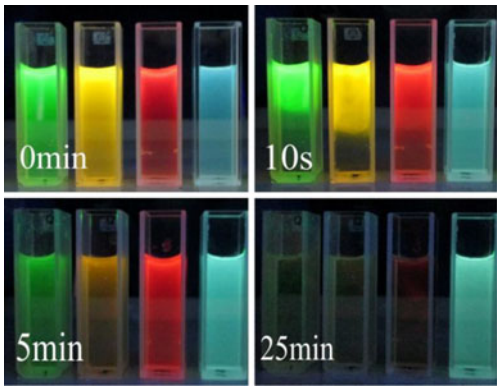

Fig. 8 FL photograghs of CdTe QDs, CdTe/CdS QD_{573}, CdTe/CdS QD_{630} and CdSeS QDs (from left to right) under the action of H_2O_2 versus the time

temporal evolution of fluorescence spectra were displayed in Fig. 7. Unexpectedly, neither of these two types of CdTe/CdS QDs showed higher stability than the naked CdTe QDs. From the photographs of the QDs under a 365 nm UV lamp (Fig. 8), we can clearly observe that, before the addition of H_2O_2, all the four types of QDs displayed bright fluorescence (CdTe QDs, green; CdTe/CdS QD_{573}, yellow; CdTe/CdS QD_{630}, red; CdSeS QDs, blue). After 25 min of the addition of H_2O_2, the fluorescence of CdTe QDs, CdTe/CdS QD_{573}, and CdTe/CdS QD_{630} quenched completely, while the fluorescence of the alloyed CdSeS QDs turned into light green, which was consistent with the result of fluorescence spectra.

In order to make clear the causes of the enhanced PL intensity and red shift of emission wavelength for the alloyed CdSeS QDs, we examined the surface change of the nature of the CdSeS nanocrystal before and after H_2O_2 treatment using X-ray photoelectron spectroscopy (XPS) and the result was shown in Figs. 9 and 10. The survey spectra of CdSeS QDs after H_2O_2 treatment showed the remained characteristic peaks of Cd 3d, Se 3d, S 2p, implying the oxidation of H_2O_2 gave no significant influence on the crystal particles. The spectra of the

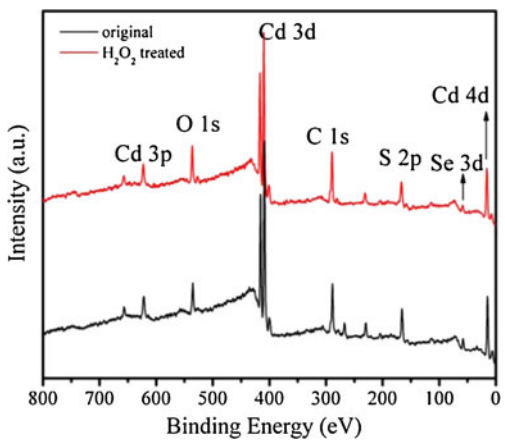

Fig. 9 Survey XPS of the original (*black line*) and H_2O_2-treated (*red line*) CdSeS QDs, respectively

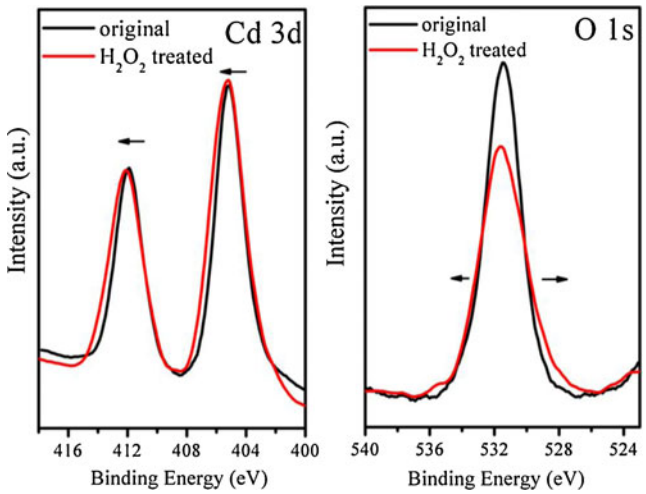

Fig. 10 XPS spectra of Cd 3d and O 1s of the original (*black line*) and H_2O_2 treated (*red line*) CdSeS QDs

Cd 3d level were slightly shifted by 0.1–0.2 eV to higher binding energy after the H_2O_2 treatment. According to the report of Jang et al., there would be a shift to lower binding energy as a CdO shell formed on the surface of CdS [35]. Since the Cd 3d peak positions for CdS and CdO are very close to each other, most researchers argue that the only way to tell the difference between the two species is in the Cd Auger peak [36]. In addition, the spectra of the O 1 s level were widened, also agreed with the report of Jang et al. [35]. These results provided evidence that in all probability a new shell CdO with a lower valence band binding energy (5.4 eV) was formed on the surface of bulk CdS (6.9 eV) after the treatment of H_2O_2, in which the CdO layers passivate the surface defects very effectively [37], and the resulting nanocrystal shows an enhanced fluorescence intensity. To further confirm our conclusion, CdSeS/CdO QDs were synthesized according to the reported literature [38]. After purification and drying, the obtained solid

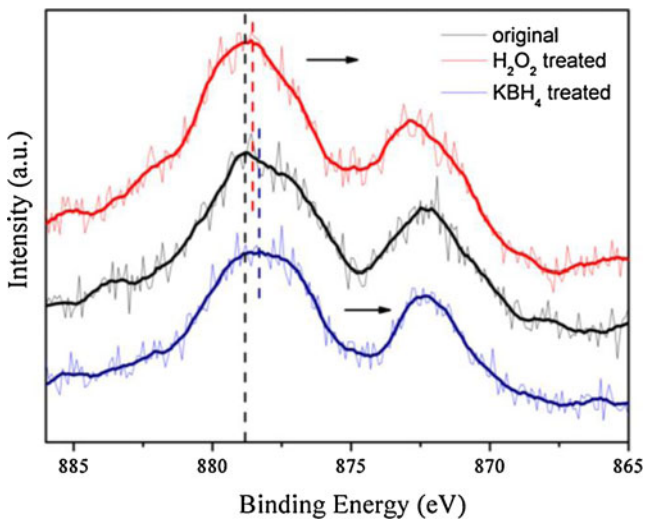

Fig. 11 XPS spectra in the Cd_{MNN} Auger region of the original (*black line*), H_2O_2-treated (*red line*) and KBH_4-treated (*blue line*) CdSeS QDs

sample was used for XPS investigation in the Cd_{MNN} Auger region to monitor the changes on the QDs surface. Figure 11 showed the results obtained for the CdSeS QDs treated by H_2O_2 and $NaBH_4$, respectively. Compared with the original CdSeS QDs, the samples treated by H_2O_2 and $NaBH_4$ displayed the peaks with a lower binding energy, which can be clearly observed by magnifying the spectra in the 875–882 eV regions. The peak position of original CdSeS QDs is 878.8 eV, while the samples treated by H_2O_2 and $NaBH_4$ are 878.5 eV and 878.3, respectively. Though the shift magnitude was not obvious, the shift trend was consistent with the previous report [39]. These results clearly suggested that the treatment of H_2O_2 correlated with the formation of CdO, as with the samples treated by $NaBH_4$. As for the samples of CdTe QDs and CdTe/CdS QDs, the oxidation of H_2O_2 made these nanocrystals particles degenerate rapidly before the CdO shell formed, even if a thick CdS layer was covered on the CdTe surface. The high tolerance of CdSeS QDs was mainly due to the quasi core shell alloyed structure and the thick CdS shell, that is, a CdSe-rich core and a thick CdS shell. The small lattice mismatch (ca. 3.6 %) between CdSe and CdS [40, 41] makes these nanocrystals much stabler than the general core-shell structured nanocrystals such as CdTe/CdS QDs.

Conclusions

A facile method was developed to synthesize CdSeS QDs through microwave irradiation in aqueous phase. UV–vis absorption spectra and fluorescence spectra showed the obtained CdSeS QDs present good optical properties. The results of XRD and XPS proved that the QDs possess a quasi core shell alloyed structure with a thick CdS shell on the surface of CdSe core, which endowed this nanomaterial high stability in an oxidative environment, which have wide applications in biolabelling and imaging.

Acknowledgments We acknowledge the financial support from the National High Technology Research and Development Program of China (863 program, No. 2007AA06Z418), the National Natural Science Foundation of China (Nos. 20577036, 20777058, 20977070), the Open Fund of Hubei Biomass-Resource Chemistry and Environmental Biotechnology Key Laboratory (HBRCEBL2011-2012005) and the Fundamental Research Funds for the Central Universities. We express our gratitude to Dr. Ying Liu, Xin-Yu Shen and Shao-Bo Mo (Center for Analysis & Testing of Wuhan University), respectively, for acquiring the XPS, XRD and TEM images.

References

1. Alivisatos AP (1996) Semiconductor clusters, nanocrystals, and quantum dots. Science 271:933–937
2. Chan WCW, Nie SM (1998) Quantum dot bioconjugates for ultrasensitive nonisotopic detection. Science 281:2016–2018
3. Michalet X, Pinaud FF, Bentolila LA, Tsay JM, Doose S, Li JJ, Sundaresan G, Wu AM, Gambhir SS, Weiss S (2005) Quantum dots for live cells, in vivo imaging, and diagnostics. Science 307:538–544
4. Muro E, Pons T, Lequeux N, Fragola A, Sanson N, Lenkei Z, Dubertret B (2010) Small and stable sulfobetaine zwitterionic quantum dots for functional live-cell imaging. J Am Chem Soc 132:4556–4557
5. Gu YP, Cui R, Zhang ZL, Xie ZX, Pang DW (2012) Ultrasmall near-infrared Ag_2Se quantum dots with tunable fluorescence for in vivo imaging. J Am Chem Soc 134:79–82
6. Mancini MC, Kairdolf BA, Smith AM, Nie S (2008) Oxidative quenching and degradation of polymer-encapsulated quantum dots: new insights into the long-term fate and toxicity of nanocrystals in vivo. J Am Chem Soc 130:10836–10837
7. Kevin MM, Andrew NM, Matthew JB, Song J, Robert JH, Joel AP (2009) Engineered nanomaterial transformation under oxidative environmental conditions: development of an in vitro biomimetic assay. Environ Sci Technol 43:1598–1604
8. Derfus AM, Chan WCW, Bhatia SN (2004) Probing the cytotoxicity of semiconductor quantum dots. Nano Lett 4:11–18
9. Aldana J, Wang YA, Peng XG (2001) Photochemical instability of CdSe nanocrystals coated by hydrophilic thiols. J Am Chem Soc 123:8844–8850
10. Ma J, Chen JY, Guo J, Wang CC, Yang WL, Xu L, Wang PN (2006) Photostability of thiol-capped CdTe quantum dots in living cells: the effect of photo-oxidation. Nanotechnology 17:2083–2089
11. Chang SQ, Dai YD, Kang B, Han W, Mao L, Chen D (2009) UV-enhanced cytotoxicity of thiol-capped CdTe quantum dots in human pancreatic carcinoma cells. Toxicol Lett 188(2):104–111
12. Sun YH, Liu YS, Vernier PT, Liang CH, Chong SY, Marcu L, Gundersen MA (2006) Photostability and pH sensitivity of CdSe/ZnSe/ZnS quantum dots in living cells. Nanotechnology 17:4469–4476
13. Xu S, Wang C, Zhang H, Wang Z, Yang B, Cui Y (2011) pH-sensitive photoluminescence for aqueous thiol-capped CdTe nanocrystals. Nanotechnology 22:315703
14. Xi L, Lek JY, Liang YN, Boothroyd C, Zhou W, Yan Q, Hu X, Chiang FBY, Lam YM (2011) Stability studies of CdSe nanocrystals in an aqueous environment. Nanotechnology 22:275706
15. Hardman R (2006) A toxicologic review of quantum dots: toxicity depends on physicochemical and environmental factors. Environ Health Perspect 114:165–172
16. Zhang Y, Mi L, Chen JY, Wang PN (2009) The environmental influence on the photoluminescence behavior of thiol-capped CdTe quantum dots in living cells. Biomed Mater 4:012001–012009
17. Hankare PP, Bhuse VM, Garadkar KM, Jadhav AD (2001) A novel method to grow polycrystalline HgSe thin film. Mater Chem Phys 71:53–57
18. Qian H, Li L, Ren J (2005) One-step and rapid synthesis of high quality alloyed quantum dots (CdSe-CdS) in aqueous phase by microwave irradiation with controllable temperature. Mater Res Bull 40:1726–1736
19. Wurth C, Grabolle M, Pauli J, Spieles M, Resch-Genger U (2011) Comparison of methods and achievable uncertainties for the relative and absolute measurement of photoluminescence quantum yields. Anal Chem 83:3431–3439
20. Crosby GA, Demas JN (1971) Measurement of photoluminescence quantum yields. J Phys Chem 75:991–1024
21. Liu YF, Xie B, Yin ZG, Fang SM, Zhao JB (2010) Synthesis of highly stable CdTe/CdS quantum dots with biocompatibility. Eur J Inorg Chem 10:1501–1506
22. He Y, Lu HT, Sai LM, Lai WY, Fan QL, Wang LH, Huang W (2006) Synthesis of CdTe nanocrystals through program process of microwave irradiation. J Phys Chem B 110:13352–13356
23. He Y, Lu HT, Sai LM, Lai WY, Fan QL, Wang LH, Huang W (2006) Microwave-assisted growth and characterization of water-dispersed CdTe/CdS core-shell nanocrystals with high photoluminescence. J Phys Chem B 110:13370–13374

24. Taniguchi S, Green M, Rizvi SB, Seifalian A (2011) The one-pot synthesis of core/shell/shell CdTe/CdSe/ZnSe quantum dots in aqueous media for in vivo deep tissue imaging. J Mater Chem 21:2877–2882
25. Rogach AL (2000) Nanocrystalline CdTe and CdTe(S) particles: wet chemical preparation, size-dependent optical properties and perspectives of optoelectronic applications. Mater Sci Eng B 69–70:435–440
26. Rogach AL, Franzl T, Klar TA, Feldmann J, Gaponik N, Lesnyak V, Shavel A, Eychmüller A, Rakovich YP, Donegan JF (2007) Aqueous synthesis of thiol-capped CdTe nanocrystals: state-of-the-art. J Phys Chem C 111:14628–14637
27. Dabbousi BO, Rodriguez-Viejo J, Mikulec FV, Heine JR, Mattoussi H, Ober R, Jensen KF, Bawendi MG (1997) (CdSe)ZnS core-shell quantum dots: synthesis and characterization of a size series of highly luminescent nanocrystallites. J Phys Chem B 101:9463–9475
28. Talapin DV, Mekis I, Götzinger S, Kornowski A, Benson O, Weller H (2004) CdSe/CdS/ZnS and CdSe/ZnSe/ZnS core-shell-shell nanocrystals. J Phys Chem B 108:18826–18831
29. Xie R, Kolb U, Li J, Basché T, Mews A (2005) Synthesis and characterization of highly luminescent CdSe-core $CdS/Zn_{0.5}Cd_{0.5}S$/ZnS multishell nanocrystals. J Am Chem Soc 127:7480–7488
30. Aldeek F, Balan L, Medjahdi G, Roques-carmes T, Malval JP, Mustin C, Ghanbaja J (2009) Enhanced optical properties of core/shell/shell CdTe/CdS/ZnO quantum dots prepared in aqueous solution. J Phys Chem C 113:19458–19467
31. Borchert H, Talapin DV, Gaponik N, McGinley C, Adam S, Lobo A, Möller T, Weller H (2003) Relations between the photoluminescence efficiency of CdTe nanocrystals and their surface properties revealed by synchrotron XPS. J Phys Chem B 107:9662–9668
32. Bao H, Gong Y, Li Z, Gao M (2004) Enhancement effect of illumination on the photoluminescence of water-soluble CdTe nanocrystals: toward highly fluorescent CdTe/CdS core-shell structure. Chem Mater 16:3853–3859
33. Pan DC, Wang Q, Jiang SC, Ji XL, An LJ (2005) Synthesis of extremely small CdSe and highly luminescent CdSe/CdS core-shell nanocrystals via a novel two-phase thermal approach. Adv Mater 17:176–179
34. Yu WW, Qu L, Guo W, Peng X (2003) Experimental determination of the extinction coefficient of CdTe, CdSe, and CdS nanocrystals. Chem Mater 15:2854–2860
35. Jang E, Jun S, Chung Y, Pu L (2004) Surface treatment to enhance the quantum efficiency of semiconductor nanocrystals. J Phys Chem B 108:4597–4600
36. Katari JEB, Colvin VL, Alivisatos AP (1994) X-ray photoelectron spectroscopy of CdSe nanocrystals with applications to studies of the nanocrystal surface. J Phys Chem 98:4109–4117
37. Dou Y, Egdell RG, Walker T, Law DSL, Beamson G (1998) N-type doping in CdO ceramics: a study by EELS and photoemission spectroscopy. Surf Sci 398:241–258
38. Ma J, Chen JY, Guo J, Wang CC, Yang WL, Cheung NH, Wang PN (2006) Improvement of the photostability of thiol-capped CdTe quantum dots in aqueous solutions and in living cells by surface treatment. Nanotechnology 17(23):5875–5881
39. Sato K, Kojima S, Hattori S, Chiba T, Ueda-Sarson K, Torimoto T, Tachibana Y, Kuwabata S (2007) Controlling surface reactions of CdS nanocrystals: photoluminescence activation, photoetching and photostability under light irradiation. Nanotechnology 18:465702
40. Krishna MVR, Friesner FLA (1991) Quantum confinement effects in semiconductor clusters. J Chem Phys 95(11):8309–8322
41. Zhan HJ, Zhou PJ, He ZY, Tian Y (2012) Microwave-assisted aqueous synthesis of small-sized, highly luminescent CdSeS/ZnS core/shell quantum dots for live cell imaging. Eur J Inorg Chem 15:2487–2493